03,07,13

Critical thickness and stresses of HgTe layers on $Hg_xCd_{1-x}Te$ substrates

© S.A. Dvoretsky[1], N.N. Mikhailov[1], R.V. Menshikov[1], V.I. Okulov[2], T.E. Govorkova[2]

[1] Rzhanov Institute of Semiconductor Physics, Siberian Branch, Russian Academy of Sciences, Novosibirsk, Russia
[2] M.N. Mikheev Institute of Metal Physics, Ural Branch, Russian Academy of Sciences, Yekaterinburg, Russia

E-mail: dvor@isp.nsc.ru

Received January 25, 2024
Revised January 25, 2024
Accepted January 26, 2024

The calculation of the critical thickness of the pseudomorphic layer and the mechanical stresses of HgTe on (013) $Hg_xCd_{1-x}Te$ substrates at growth temperatures of 120, 150 and 180°C for two dislocation sliding systems was carried out. It was found that the critical thickness of HgTe varies from 40–60 to 1200–1800 nm with a change in x from 0 to 0.9. Mechanical stresses due to the mismatch of the lattice parameters of the HgTe/$Hg_xCd_{1-x}Te$ heteroparticle vary in the range from 6 to 125 MPa with a change in x and weakly depend on temperature. Mechanical stresses during cooling due to the discrepancy between the coefficients of thermal expansion ranged from −1 to −7 MPa. These results make it possible to predict mechanical stresses in various instrument structures based on the HgTe/$Hg_xCd_{1-x}Te$ heteropair.

Keywords: critical thickness, stresses, composition, HgTe, $Hg_xCd_{1-x}Te$, lattice parameter, coefficient of thermal expansion.

DOI: 10.61011/PSS.2024.02.57916.9

1. Introduction

Single-crystals and heteroepitaxial layers based on gapless compounds HgSe and HgTe attract special attention of researchers due to their unusual physical properties, which are determined by their unique electronic structure and high electrical parameters. The electron concentration is less than $10^{15}\,cm^{-3}$ for HgTe and about $10^{17}\,cm^{-3}$ for HgSe. The electron mobility reaches values of more than $10^5\,cm^2/V\cdot s$. Thus, when studying bulk HgSe single-crystals doped with transition $3d$-metals (Fe, Co, Ni) of extremely low concentrations (< 1 at.%), were discovered, and the features of electronic properties associated with the manifestations of abnormalities in the temperature and concentration dependences of kinetic (electron concentration, mobility, Hall coefficient) and thermodynamic coefficients (heat capacity, speed and absorption of ultrasound, magnetic susceptibility) were studied in detail. It was identified that all the observed effects are due to the hybridization of the electronic states of the d-impurity and the conduction band of the crystal, and are described under the developed theory of resonant scattering and spontaneous spin polarization [1–7]. One of the actively developing directions of studies in this area is associated with the study of new quantum effect — spontaneous spin magnetism of donor conduction electrons [7]. Magnetism of this type was experimentally discovered in bulk single-crystals HgSe:Fe(Co) with extremely low concentration of d-impurities (< 1 at.%) both at low ~ 5 K [8–10], and at room temperatures [11]. The electronic structure of such systems is gapless crystalline matrix HgSe and a conduction band filled with donor electrons of impurity atoms. Spontaneous spin magnetism of new type (without inter-impurity interaction) is observed under the condition of an extremely low concentration of d-impurities (< 1 at.%). In this case, in the conduction band of the HgSe crystal matrix a system of donor electrons is formed, the states of which, under the influence of strong spin-dependent exchange inter-electron interaction, under the conditions of the initial polarization of electrons of impurity atoms, create complete spontaneous spin polarization of such system. In this case, the impurity states hybridize with states of the conduction band, which is also a necessary condition for the occurrence of spontaneous spin polarization of new type. However, it is quite difficult to control such properties when concentration of d-impurities in crystals changes. The development of epitaxial technologies made it possible to consider layers to create magnetic materials with low concentration of magnetic impurity.

Interest in studies of heteroepitaxial layers based on HgSe and HgTe doped with $3d$-impurities opens up wide opportunities for both further study of impurity magnetism of new type (in the transition from bulk single-crystals to layers) and for the discovery of new physical properties of such structures. It was shown that HgSe layers grown on (001)ZnTe/GaAs substrates during Fe doping to concentration greater than $5\cdot10^{18}\,cm^{-3}$ showed a significant increase in mobility up to $2.7\cdot10^5|\,cm^2/V\cdot s$ compared to undoped layers [12,13]. The authors associated the observation of this effect with Fermi level pinned to Fe donor located in the conduction band, which was noted

for HgSe:Fe crystals [14]. However, such result was not obtained in further studies, which was determined by the low structural perfection of the HgSe:Fe layers associated with the low growth temperature of less than 120°C [15–18]. The higher growth temperatures allows to increase the crystal structure perfection. It was proposed to consider the growth of HgTe layers upon doping with 3*d*-elements to different concentrations as a promising material for creating a magnetic semimetal. It was shown that HgTe layers grown at ~ 180°C on various substrates are of high quality [19–21], which made it possible to create various low-dimensional structures based on quantum wells [22-30].

To create a material upon growing HgTe layers by MBE with magnetic properties when doped with impurity Fe atoms on (013)$Cd_{1-x}Hg_xTe$/ZnTe/GaAs, it is necessary to consider the influence of such a complex substrate on the expected structural quality, arising and residual stresses, depending on the layer thickness and growth temperature.

Structural quality is mainly determined by dislocation density. To minimize the density of dislocations arising during the growth process, it is necessary to determine the critical thickness of the pseudomorphic layer (h_c), in which the generation of mismatch dislocations (MDs) does not occur. The h_c depends on the mismatch between the lattice constants of the conjugation materials of the grown layer and the substrate at growth temperature and orientation. When HgTe layer thickness exceeds h_c, the generated MDs will lead to a deterioration in the structural quality. Mechanical stresses that arise in layers with thickness h_c will be determined by the mismatch between the lattice constants during growth and the coefficients of thermal expansion during cooling. The magnitude of mechanical stress will decrease with thickness increasing.

Thus, when growing HgTe layers on complex multilayer substrate (013)$Cd_{1-x}Hg_xTe$/CdTe/ZnTe/GaAs, it is necessary to analyze the parameters h_c and mechanical stresses that will determine the processes of Fe atoms incorporation during doping and their electronic state.

The paper presents an analysis of the critical thickness h_c of HgTe layers and stresses during growth on relaxed (013)$Cd_{1-x}Hg_xTe$/CdTe/ZnTe/GaAs substrates dependence on the composition x at different growth temperatures and subsequent cooling to room temperature. The influence of the thickness of the HgTe layer on the magnitude of residual stresses was assessed.

2. Analysis

2.1. Calculation of the critical thickness of the pseudomorphic layer

The critical thickness of the pseudomorphic layer h_c was calculated using the formula obtained in accordance with the Matthews model [31]:

$$h_c = (b/\cos\lambda)(1 - \nu\cos 2\alpha)[1 + \ln(h_c/b)]/[8\pi(1+\nu)f], \quad (1)$$

where α — the angle between the Burgers vector b and the dislocation line, λ — the angle between the Burgers vector and the direction lying in the interface perpendicular to MD, ν — Poisson's ratio in an isotropic solid and $f = (a_l - a_s)/a_s$ — mismatch parameter equal to the relative difference in the lattice constants of layer (a_l) and substrate (a_s). Expression (1) was obtained as a result of the equilibrium thermodynamic approach and is valid only as a certain limit, to which the system will tend to under infinite hold-up. In actual situation of film growth at finite rate, the influence can be exerted by kinetic factors associated with the mechanism of MD introduction [32]. For the case of heteroepitaxy on vicial surfaces, the introduction of MDs belonging to slip systems $(a/2)\langle 110\rangle\{111\}$ occurs within the 12 dislocation systems (DS) [33]. In the case of heteroepitaxy of HgCdTe layers on (013)CdTe/ZnTe/GaAs substrate the parameters of these DSs are given in [34]. Experimental results obtained by transmission microscopy showed that for layers $Hg_{0.7}Cd_{0.3}Te$ when growing on (013)CdTe MDs are introduced at thicknesses comparable to the calculated values h_c for DS 1, 2 and 3, 4, for which the angles α and λ are 79.1 deg. and 44.2 deg., 40.9 deg. and 61.4 deg. respectively.

We simulated h_c of HgTe layer during growing on the surface (013)$Hg_xCd_{1-x}Te$ using formula (1) with data on angles α and λ for DS 1, 2 and 3, 4 in the interval $x = (0{-}0.9)$ with a step of 0.1. Burgers vector $b = a_{HgTe}/2$ in the direction [110] and $[\bar{1}10]$ for the system 1, 2 and 3,4, respectively. The calculation was carried out for growth temperatures of 120, 150 and 180°C. The mismatch of lattice constants $f = (a_{HgTe} - a_{Hg_xCd_{1-x}Te})/a_{Hg_xCd_{1-x}Te}$ is determined at the indicated temperatures (T) using the formula [35]:

$$a(x,T) = 6.4614 + 0.008x + 0.0168x^2 - 0.0057x^3 - 0.0095 + 2.613\cdot 10^{-5}T + 1.131\cdot 10^{-8}T. \quad (2)$$

Poisson's ratios ν were obtained by calculating the elastic constants for the growth temperature.

2.2. Calculation of residual stresses after growth in HgTe layers

The expression for calculating the mechanical stresses ($\sigma_{mech.}$) of the layer includes the stresses associated with the mismatch of lattice constants ($\sigma_{misf.}$) that arise during the growth, and the mismatches in the thermal expansion coefficients that arise when the grown structure is cooled after growing ($\sigma_{therm.}$):

$$\sigma_{mech.} = \sigma_{misf.} + \sigma_{therm.}. \quad (4)$$

Table 1. Values of elastic constants and temperature coefficients

Compound	Elastic constants, GPa			α_C, GPa/K		
	C_{11}	C_{12}	C_{44}	C_{11}	C_{12}	C_{44}
CdTe	53.6	37.0	20.1	0.011	0.009	0.002
HgTe	54.1	37.4	20.8	0.020	0.016	0.006

The σ_{mismatch} was calculated using the equation proposed in [36]

$$\sigma_{\text{misf.}} = \frac{E f(h_c/h)}{1-\nu}, \tag{5}$$

where E — Young's modulus, h_c — thickness of the pseudomorphic layer, h — thickness of the grown layer.

This expression determines the magnitude of the mechanical stress on the thickness, which has maximum value at $h = h_c$ and at $h > h_c$ decreases in inverse proportion to the thickness of the layer. Young's modulus was calculated using the formula [37]:

$$\frac{1}{E} = \frac{C_{11}+C_{12}}{(C_{11}-2C_{12})} + \left(\frac{1}{C_{44}} - \frac{2}{C_{11}-C_{12}}\right) \times (n_X^2 n_Y^2 + n_X^2 n_Z^2 + n_Y^2 n_Z^2), \tag{6}$$

where C_{11}, C_{12} and C_{44} — elastic constants; n_X, n_Y and n_Z — direction cosines.

The elastic constants C_{ij} at growth temperatures T were calculated under the assumption of a linear dependence of elastic constants on temperature in accordance with [38]:

$$C_{ij}(T) = C_{ij}(300) + \alpha_C(300 - T). \tag{7}$$

The values of the elastic constants C_{ij} and their temperature coefficients α_C are given in Table 1.

Value of parameter ν for HgTe layers at the growth temperature was determined according to method in [38]:

$$\nu^{=} = \frac{3B - 2\mu}{2(3B + \mu)}, \tag{8}$$

where $B = \frac{C_{11}+2C_{12}}{3}$ — bulk modulus of elasticity; $\mu = \frac{C_{11}-C_{12}+C_{44}}{3}$ — shear modulus.

Calculations showed that ν was equal to 0.366, 0.365 and 0.364 at temperatures 120, 150 and 180°C, respectively.

The residual stresses at HgTe layer in the structure $HgTe/Hg_xCd_{1-x}Te/CdTe/ZnTe/GaAs$ during cooling from the growth temperature to room temperature were calculated using the formula for

$$\sigma_{\text{therm}} = \frac{E\Delta\alpha_T\Delta T}{(1-\nu)}, \tag{9}$$

where $\Delta\alpha = \alpha_{\text{HgTe}} - \alpha_{\text{GaAs/substrate}}$, α_{HgTe} and α_{GaAs} — thermal expansion coefficients of HgTe and GaAs, ΔT — temperature range during cooling from growth temperature to room temperature. Stress calculations for multilayer structure can be performed for each layer [39].

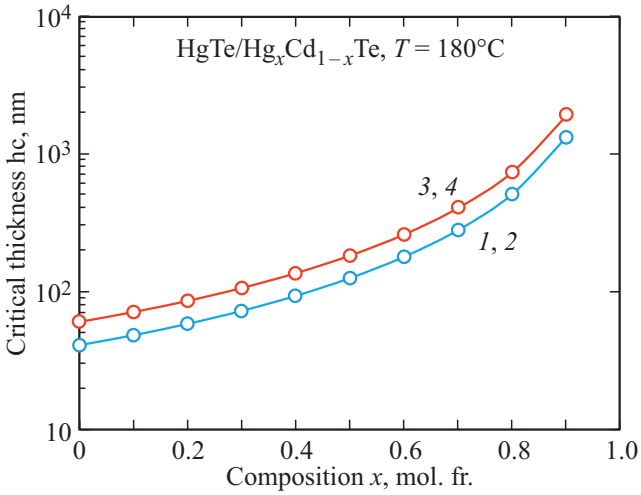

Figure 1. Dependence of critical h_c of HgTe layer at growth temperature 180°C.

3. Discussion of results

Figure 1 shows dependence of critical thickness h_c of HgTe layer in heteropair $HgTe/Hg_xCd_{1-x}Te$ on x at temperature 180°C for slip DS 1, 2 and 3, 4.

As follows from the data presented, with increase in x the thickness h_c increases significantly, but weakly depends on temperature. This is due to the large change in the mismatch between the lattice constants of HgTe and $Hg_xCd_{1-x}Te$ with changes in composition x and weak change with change in temperature, which are determined by the lattice constants as follows from relation (2). Note that data obtained at $x = 0$ practically do not match with the calculation h_c in [36] for the heteropair $Hg_xCd_{1-x}Te/CdTe$.

Table 2 shows values h_c of HgTe layer for the heteropair $HgTe/Hg_xCd_{1-x}Te$ for temperatures 120, 150 and 180°C upon change in composition x from 0 to 0.9 with step 0.1.

Critical thickness h_c for DS 1, 2 is by 1.5 times lower that in case of DS 3, 4 for all growth temperatures, and is 40–60 nm and 1200–1900 nm for $x = 0$ and $x = 0.9$, respectively. For both DSs a weak temperature dependence is observed h_c. Note that kinetic limitations of the processes of MD introduction can lead to increase in h_c, which can exceed the calculated values by ~ 2 times for the growth temperature ~ 180°C, as shown for the heteropair $Hg_{0.7}Cd_{0.3}Te/CdTe$ at the beginning of the dislocations introduction [34] observed at thickness of $Hg_{0.7}Cd_{0.3}Te$ layer 75 nm.

When growing HgTe layer on CdTe substrate with thickness less than h_c, the crystal lattice constant of HgTe layer will have the value of CdTe lattice constant. The surface morphology of HgTe/CdTe layers with thickness less than h_c will have roughness at the nanometer level. When the thickness of HgTe layers exceeds h_c, the surface morphology of the layers will gradually change from island-like to their subsequent merging and smoothing of the

Table 2. Critical thickness of pseudomorphic HgTe layer for heteropair HgTe/$Hg_xCd_{1-x}Te$ for two DSs 1, 2 and 3, 4

Substrate composition x, mol.%	Critical thickness of pseudomorphic HgTe layer, h_c, nm					
	Growth temperature, °C		Growth temperature, °C		Growth temperature, °C	
	120		150		180	
	Slip system of dislocations		Slip system of dislocations		Slip system of dislocations	
	1, 2	3, 4	1, 2	3, 4	1, 2	3, 4
0	37.0	54.7	38.6	57.0	40.8	60.2
0.1	43.7	64.5	45.7	67.3	48.2	71.0
0.2	52.9	77.8	55.2	81.2	58.3	85.6
0.3	65.7	96.4	68.6	100.6	72.4	106.1
0.4	84.6	123.7	88.3	129.0	93.1	136.0
0.5	113.8	165.9	118.7	173.0	125.2	182.3
0.6	162.7	236.4	169.7	246.5	178.8	259.6
0.7	254.6	368.0.	265.4	384.2	279.5	404.5
0.8	465.0	670.5	484.5	698.4	510.0	734.9
0.9	1205.0	1728.1	1254.7	1799.1	1319.7	1891.8

Table 3. Stress of pseudomorphic layers HgTe in heteropair HgTe/$Hg_xCd_{1-x}Te$

Substrate composition x, mol.%	Stresses HgTe in heteropair HgTe/$Hg_xCd_{1-x}Te$, σ_{misf} MPa		
	Growth temperature, °C	Growth temperature, °C	Growth temperature, °C
	120	150	180
0	125.8	124.6	123.5
0.1	109.7	108.7	107.7
0.2	93.8	92.9	92.1
0.3	78.3	77.6	76.9
0.4	63.4	62.8	62.3
0.5	49.4	48.9	48.5
0.6	36.4	36.1	35.8
0.7	24.8	24.6	24.4
0.8	14.7	14.6	14.4
0.9	6.4	6.3	6.2

surface. Experimental studies will make it possible to determine the required thickness of the continuous HgTe layer with minimal surface roughness. Doping with Fe to less than 1 at.% shall not have a significant effect on the surface morphology.

When growing HgTe layer on substrates with $x \sim 0.8-0.9$, the thickness h_c is more than 1000 nm (1 μm). The lattice constant of HgTe layer will have a value slightly different from the lattice constant of the HgTe crystal. The surface morphology of such HgTe/$Cd_{0.1}Hg_{0.9}Te$ layers will have roughness at the nanometer level.

Change in the composition of the substrate x in case of the growth of HgTe layers will make it possible to change the lattice constant of the HgTe layers and the state of the surface morphology.

Figure 2 shows the dependence of the stresses caused by the mismatch of lattice constants $\sigma_{misf.}$ in HgTe layer up to h_c thick on the composition of $Hg_xCd_{1-x}Te$ at 180°C.

As can be seen from the above data, the stresses decrease with increase in composition x, which is associated with a decrease in the mismatch between the lattice constants of HgTe and $Hg_xCd_{1-x}Te$ in the heteropair HgTe/$Hg_xCd_{1-x}Te$.

Table 3 shows the stresses $\sigma_{misf.}$ in HgTe layers at temperatures 120, 150 and 180°C.

When growing HgTe layer on CdTe substrate, the stresses are of 123−125 MPa when the growth temperature changes from 180°C to 120°C. When the thickness of HgTe layer increases during growth on CdTe exceeds the critical value by $\sim$ 20 times the introduction of MD will lead to stress decreasing inversely proportional to the thickness of the layer, as follows from expression (5), and will be $\sim$ 6 MPa for all temperatures.

When growing HgTe layer on substrates with $x \sim 0.9$, the stress in HgTe layer 1000 nm thick will be 6 MPa at growth temperatures of 120−180°C.

Table 4. Stresses $\sigma_{term.}$ in HgTe layer after cooling from growth temperature to room temperature

Coefficient of thermal expansion, $\Delta\alpha_T$, 1/T	Stresses of HgTe layer during cooling $\sigma_{therm.}$, MPa		
	Growth temperature, °C	Growth temperature, °C	Growth temperature, °C
	120	150	18
for $\alpha_{HgTe} = 0.00000485$ 1/T [40]	−5.1	−6.6	−6.8
for $\alpha_{HgTe} = 0.00000545$ 1/T [41]	−1.0	−1.3	−1.4

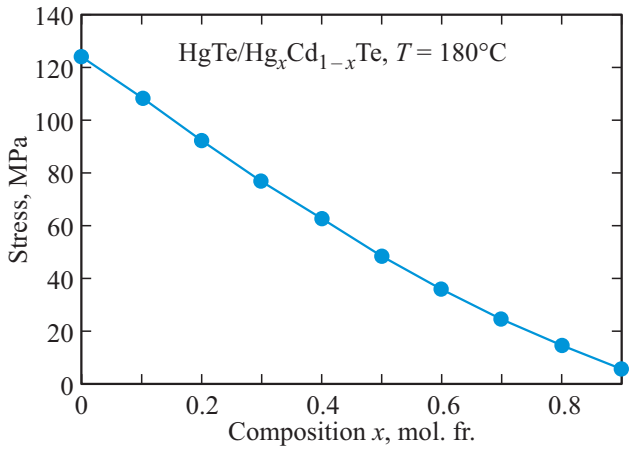

Figure 2. Stresses of the pseudomorphic HgTe layer in the heteropair HgTe/$Hg_xCd_{1-x}Te$ vs. composition x at temperature of 180°C.

Thus, during the growth of HgTe layer on CdTe and $Hg_{x\,0.9}Cd_{0.1}Te$ substrates the layers HgTe will be obtained with the same residual stresses caused by the mismatch of lattice constants, but with different structural perfection — layers with introduced MDs and pseudomorphic layers.

The choice of the substrate composition, the required thickness of HgTe layer and the growth temperature will make it possible to obtain the material with stresses changing in a wide range of values and different structural perfection.

Table 4 shows data on the stresses in HgTe layer in HgTe/$Hg_xCd_{1-x}Te$/CdTe/ZnTe/GaAs structure after cooling from the growth temperature to room temperature (300 K). The values of the thermal expansion coefficients for HgTe and GaAs were taken from publications and amounted to $\alpha_{HgTe} = 0.00000485$ 1/T [40], $\alpha_{HgTe} = 0.00000545$ 1/T [41], and $\alpha_{GaAs} = 0.0000056$ 1/T [42].

The obtained stress values during cooling from growth temperatures 120, 150 and 180°C to room temperature due to the mismatch of thermal cooling coefficients are comparable to the stresses determined by the difference in lattice constants at the same growth temperatures using data from [40]. For the mismatch data of thermal cooling coefficients from [41], the low value of stresses during cooling from growth temperatures to room temperature was obtained. The sign of the stresses indicates compression of HgTe layers during cooling.

Thus, we can expect that the total stresses $\sigma_{mech.}$ of HgTe layers after growth, determined by formula (4), will be absent in grown HgTe layers 1000 nm thick or will have a weak stretch, which stress will be ~ 5 MPa when mating HgTe layers with $Hg_{0.9}Cd_{0.1}Te$ and with CdTe.

The simulation of the critical thickness h_c of layers and stresses $\sigma_{mech.}$ allows us to analyze the possible state of the crystal structure of HgTe layers during their growth and doping with iron.

4. Conclusion

The parameters of HgTe layers were simulated when growing by molecular beam epitaxy (MBE) on the surface $Hg_xCd_{1-x}Te$ within the structure (013)$Hg_xCd_{1-x}Te$/CdTe/ZnTe/GaAs for subsequent doping with Fe.

We calculated and obtained the values of the critical thickness (h_c) of the pseudomorphic HgTe layer when growing on $Hg_{1-x}Cd_xTe$ substrates with different cadmium contents and at different growth temperatures. It is shown that the value h_c is determined by the mismatch of lattice constants and weakly depends on temperature.

A calculation was carried out, and the stresses of HgTe layers in the heteropair HgTe/$Hg_{1-x}Cd_xTe$ were obtained depending on the magnitude of the mismatch of lattice constants at different temperatures and upon cooling to room temperature. It was found that stresses are determined by the mismatch of lattice constants, practically independent of the growth temperature and lead to stretching of HgTe lattice. Cooling results in low compressive stresses.

The data obtained make it possible to assess the structural state of HgTe layers and determine the conditions for their growth.

Funding

This study was supported by a grant from the Russian Science Foundation, project No. 23-22-00126, https://rscf.ru/project/23-22-00126/

Conflict of interest

The authors declare that they have no conflict of interest.

References

[1] V.I. Okulov, T.E. Govorkova, V.V. Gudkov, I.V. Zhevstovskikh, A.V. Korolyev, A.T. Lonchakov, K.A. Okulova, E.A. Pamyatnykh, S.Yu. Paranchich. Low Temp. Phys. **33**, 207 (2007).

[2] T.E. Govorkova, I.V. Zhevstovskikh, A.T. Lonchakov, V.I. Okulov, K.A. Okulova, S.M. Podgornykh, S.B. Bobin, V.V. Deryushkin, L.D. Paranchich. Low Temp. Phys. **43**, 508 (2017).

[3] A.T. Lonchakov, V.I. Okulov, T.E. Govorkova, M.D. Andrichuk, L.D. Paranchich. JETP Lett. **96**, 405 (2012).

[4] V.I. Okulov, T.E. Govorkova, I.V. Zhevstovskikh, A.T. Lonchakov, K.A. Okulova, E.A. Pamyatnykh, S.M. Podgornykh, M.D. Andriichuk, L.D. Paranchich. Low Temp. Phys. **39**, 384 (2013).

[5] T.E. Govorkova, A.T. Lonchakov, V.I. Okulov, M.D. Andrichuk, A.F. Gubkin, L.D. Paranchich. Low Temp. Phys. **41**, 154 (2015).

[6] V.I. Okulov. Low Temp. Phys. **30**, 897 (2004).

[7] V.I. Okulov, E.A. Pamyatnykh, V.P. Silin. Low Temp. Phys. **37**, 798 (2011).

[8] T.E. Govorkova, V.I. Okulov. Low Temp. Phys. **44**, 1221 (2018).

[9] T.E. Govorkova, V.I. Okulov, K.A. Okulova. Low Temp. Phys. **45**, 234 (2019).

[10] T.E. Govorkova, V.I. Okulov. Phys. Solid State **64**, 58 (2022).

[11] T.E. Govorkova, V.I. Okulov, E.A. Pamyatnykh, V.S. Gaviko, V.T. Surikov. Bull. Russ. Acad. Sci. Phys. **87**, 735 (2023).

[12] Th. Widmer, D. Schicora, G. Hendorfer, S. Luther, W. Jantsch, K. Lischka, M.v. Ortenberg. Mater. Sci. Forum **182–184**, 395 (1995).

[13] D. Schikora, Th. Widmer, C. Prott, K. Lischka, P. Scäfer, G. Machel, S. Luther, M. von Ortenberg. Solid State Electron. **40**, 63 (1996).

[14] F.S. Pool, J. Kossut, U. Debska, R. Reifenberger. Phys. Rev. B **35**, 3900 (1987).

[15] D. Schikora, Th. Widmer, K. Lischka, P. Scäfer, G. Machel, S. Luther, M. von Ortenberg. J. Cryst. Growth **159**, 959 (1996).

[16] L. Parthier, H. Wißmann, S. Luther, G. Machel, M. Schmidbauer, R. Kiihler, M. von Ortenberg. J.Cryst. Growth **175/176**, 642 (1997).

[17] D. Schikora, T. Widmer, K. Lischka, P. Schäfer, G. Machel, S. Luther, M. von Ortenberg. Phys. Rev. B **52**, 12072 (1995).

[18] C.R. Becker, L. He, S. Einfeldt, Y.S. Wu, H. Heinke, S. Oehling, R.N. Bicknell-Tassius, G. Landwehr. J. Cryst. Growth **127**, 331 (1993).

[19] J.P. Faurie, S. Sivananthan, M. Boukerche, J. Reno. Appl. Phys. Lett. **45**, 1307 (1984).

[20] E. Selvig, C.R. Tonheim, K.O. Kongshaug, T. Skauli, T. Lorentzen, R. Haakenaasen. J. Vac. Sci. Technol. B **25**, 1776 (2007).

[21] E. Selvig, C.R. Tonheim, T. Lorentzen, K.O. Kongshaug T. Skauli, R. Haakenaasen. J. Electron. Mater. **37**, 1444 (2008).

[22] M. Kónig, S. Wiedmann, A. Roth, H. Buhmann, L.W. Molemkamp, X.L. Qi, S.C. Zhang. Science **318**, 766 (2007).

[23] Z.D. Kvon, E.B. Olshanetsky, D.A. Kozlov, N.N. Mikhailov, S.A. Dvoretskii. JETP Lett. **87**, 502 (2008).

[24] C. Brune, C.X. Liu, E.G. Novik, E.M. Hankiewicz, H. Buhmann, Y.L. Chen, X.L. Qi, Z.X. Shen, S.C. Zhang, L.W. Molemkamp. Phys. Rev. Lett. **106**, 126803 (2011).

[25] E.B. Olshanetsky, Z.D. Kvon, S.S. Kobylkin, D.A. Kozlov, N.N. Mikhailov, S.A. Dvoretsky, J.C. Portal. JETP Lett. **93**, *9*, 526 (2011).

[26] S.A. Dvoretsky, N.N. Mikhailov, Yu.G. Sidorov, V.A. Shvets, S.N. Danilov, B. Wittmann, S.D. Ganichev. J. Electron. Mater. **39**, *7*, 918 (2010).

[27] M.V. Yakunin, A.V. Suslov, M.R. Popov, E.G. Novik, S.A. Dvoretsky, N.N. Mikhailov. Phys. Rev. B **93**, 085308 (2016).

[28] S.V. Gudina, Yu.G. Arapov, V.N. Neverov, S.M. Podgornykh, M.R. Popov, N.G. Shelushinina, M.V. Yakunin, S.A. Dvoretsky, N.N. Mikhailov. Phys. Status Solidi C **13**, *7–9*, 473 (2016).

[29] S.V. Morozov, V.V. Rumyantsev, M.A. Fadeev, M.S. Zholudev, K.E. Kudryavtsev, A.V. Antonov, A.M. Kadykov, A.A. Dubinov, N.N. Mikhailov, S.A. Dvoretsky, V.I. Gavrilenko. Appl. Phys. Lett. **111**, *19*, 192101 (2017).

[30] M.A. Fadeev, V.V. Rumyantsev, A.M. Kadykov A.A. Dubinov, A.V. Antonov, K.E. Kudryavtsev, S.A. Dvoretskii, N.N. Mikhailov, V.I. Gavrilenko, S.V. Morozov. Opt. Express **26**, *10*, 12755 (2018).

[31] J.W. Matthews. J. Vac. Sci. Technol. **12**, 126 (1975).

[32] Yu.B. Bolkhovityanov, Oleg P.Pchelyakov, S.I. Chikichev. Physics Uspekhi, **44**, 655 (2001).

[33] E.M. Trukhanov, A.V. Kolesnikov, I.D. Loshkarev. J. Surf. Investig. **8**, 502 (2014).

[34] Y.G. Sidorov, M.V. Yakushev, V.S. Varavin, A.V. Kolesnikov, E.M. Trukhanov, I.V. Sabinina, and I.D. Loshkarev. Phys. Solid State **57**, 2151 (2015).

[35] P. Capper. EMIS Datareviews Ser. N 10. INSPEC, London (1994). P. 41.

[36] M. Carmody, J.G. Pasko, D. Edwall, R. Bailey, J. Arias, M. Groenert, L.A. Almeida, J.H. Dinan, Y. Chen, G. Brill, N.K. Dhar. J. Electron. Mater. **35**, *6*, 1417 (2006).

[37] I.V. Kurilo, V.P. Alekhin, I.O. Rudyi, S.I. Bulychev, L.I. Osypyshin. Phys. Status Solidi A **163**, 47 (1997).

[38] M.A. Berding, W.D. Nix, D.R. Rhiger, S. Sen, A. Sheer. J. Electron. Mater. **29**, 676 (2000).

[39] A.R. Shgurov, A.V. Panin. Tech. Phys. **65**, 1881 (2020).

[40] T. Skauli, R. Haakenaasen, T. Colin. J. Cryst. Growth **241**, 39 (2002).

[41] P. Gergaud, A. Jonchére, B. Amstatt, X. Baudry, D. Brellier, P. Ballet. J. Electron. Mater. **41**, 2694 (2012).

[42] V.K. Yang, M. Groenert, C.W. Leitz, A.J. Pitera, M.T. Currie, E.A. Fitzgerald. J. Appl. Phys. **93**, *7*, 3859 (2003).

Translated by I.Mazurov